Synthesis, X-ray Studies and Magnetic Properties of Dinuclear Ni^{II} and Cu^{II} Complexes Bridged by the Azo-2,2′-bipyridine Ligand

Cristian S. Campos-Fernández,[a] José R. Galán-Mascarós,*[b] Bradley W. Smucker,[a] and Kim R. Dunbar*[a]

Keywords: Magnetic properties / Azo compounds / Nickel / Copper

Two new paramagnetic transition metal complexes that contain the bridging ligand azo-2,2′-bipyridine (abpy) have been prepared and characterized by X-ray crystallography and magnetic susceptibility measurements. The compound $[Ni_2(\mu\text{-abpy})(CH_3CN)_2(NO_3)_4]\cdot 2CH_3CN$ (**1**·2CH_3CN) crystallizes in the triclinic space group $P\bar{1}$ with a = 8.290(5) Å, b = 8.343(5) Å, c = 11.180(5) Å, α = 105.36(3)°, β = 94.39(3)°, γ = 107.56(3)°, V = 700.5(7) Å^3 and Z = 1. The related salt $[Cu_2(\mu\text{-abpy})(CH_3CN)_8][BF_4]_4$ (**2**) crystallizes in the triclinic space group $P\bar{1}$ with a = 10.240(2) Å, b = 10.597(2) Å, c = 10.712(2) Å, α = 64.23(3)°, β = 78.21(3)°, γ = 78.57(3)°, V = 1026.7(3) Å^3 and Z = 1. Solutions of **2** eventually produce the polymeric Cu^I compound $\{[Cu(\mu\text{-abpy})][BF_4]\}_\infty$ (**3**) which was also crystallographically characterized: monoclinic space group $P2_1/n$, with a = 9.295(2) Å, b = 9.541(2) Å, c = 13.486(3) Å, β = 91.58(3)°, V = 1195.5(4) Å^3 and Z = 4. The magnetic properties of these dinuclear paramagnetic complexes have been studied in detail, and have provided an opportunity for probing the ability of this ligand to mediate magnetic exchange interactions between paramagnetic metal centers. Compound **1** exhibits antiferromagnetic exchange interactions (J = −7.5 cm^{-1}) whereas the magnetic interactions in compound **2** were found to be negligible.

Introduction

The redox and spin-state properties of transition metal complexes render them attractive candidates for applications in many areas including molecular electronics, information recording, and catalysis.[1−3] One approach for the preparation of metal compounds with enhanced properties is to use organic ligands that engage in π-interactions with metal ions. In our quest for such ligands to use in assemblies of paramagnetic metal ions, we recently prepared families of transition metal complexes based on the nitrogen heterocyclic ligands 3,6-bis(2-pyridyl)-1,2,4,5-tetrazine (bptz)[4,5] and 1,4,5,8,9,11-hexaazatriphenylene (HAT).[6] By controlling parameters such as the identity of the anions in reactions of metal cations with bptz, for example, we have demonstrated that one can deliberately prepare different cyclic oligomers, such as molecular squares[4,6] or molecular pentagons.[5] Despite the interesting supramolecular aspects of this work, our main goal, namely to induce magnetic interactions between the paramagnetic metal ions in these molecules, was not achieved. This is primarily due to the fact that the bptz and HAT bridging ligands position the metal centers at greater distances than is reasonable for the observation of strong magnetic coupling. In considering this problem, we turned to the azo-2,2′-bypyridine (abpy) ligand (Figure 1) which offers several obvious advantages over the previous ligands, one of which is the fact that it is possible to prepare the one-electron reduction species $abpy^{-\cdot}$ to use as a radical bridging ligand. It is well-known that the use of a paramagnetic bridge is advantageous for improving magnetic superexchange between metal centers,[7−19] but we reasoned that even the diamagnetic neutral form of abpy may allow for magnetic interactions due to the short distances between metal ions afforded by the azo bridging group. Monomeric and dimeric complexes of this ligand with 3d metals have been reported,[20] although their magnetic properties have only been briefly described for several monomeric complexes and for the dimers $[(\mu\text{-abpy})Co_2Cl_4]$ and $[(\mu\text{-abpy})Co_2(hfacac)_4]$ [hfacac = bis(hexafluoroacetylacetonate)].[21,22] We postulated that the shorter path could give rise to stronger magnetic interactions between spin carriers than the previously mentioned polynitrogen ligands, which require a four-atom separation between metals. There is, in fact, evidence that the abpy ligand allows for electronic communication between metals,[23−25] as illustrated by the redox behavior of the compound [(bpy)Ru(μ-abpy)Ru-

[a] Department of Chemistry, Texas A&M University,
P. O. Box 30012, College Station, Texas 77842-3012, USA
Fax: (internat.) + 1-979/845-7177
E-mail: dunbar@mail.chem.tamu.edu
[b] Instituto de Ciencia Molecular, Universidad de Valencia,
Dr. Moliner, 50, Burjassot 46100, Spain
Fax: (internat.) + 34-96/386-4859
E-mail: jose.r.galan@uv.es

(bpy)][PF_6]$_4$ which exhibits a comproportionation constant K_c of more than 10^8. This value corresponds to a class III delocalized system on the Robin and Day scale.[26]

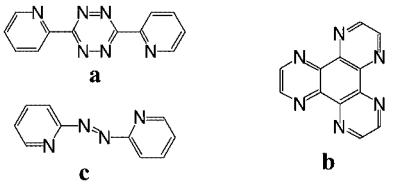

Figure 1. Scheme of the polynitrogen ligands: (a) 3,6-bis(2-pyridyl)-1,2,4,5-tetrazine (bptz); (b) 1,4,5,8,9,11-hexaazatriphenylene (HAT); (c) azo-2,2′-bipyridine (abpy)

With all the aforementioned premises in mind, we embarked on a study of the nature of azo-2,2′-bypyridine (abpy) as a bridge between magnetic ions of the first row transition metals. Three compounds were isolated and characterized in this work, namely two magnetic dinuclear compounds of Ni^{II} and Cu^{II}, and a diamagnetic Cu^{I} polymer.

Results and Discussion

Syntheses

The reactions between Ni^{II} and Cu^{II} ions with abpy proceed instantaneously in acetonitrile to afford the products [Ni_2(abpy)(CH_3CN)$_2$(NO_3)$_4$] (**1**) and [Cu_2(abpy)(CH_3CN)$_8$][BF_4]$_4$ (**2**) in good yields. In marked contrast to previous reports, which concluded that a large activation barrier exists for the coordination of a second metal center after the first metal is bound,[17] the formation of the dinuclear species is facile in these cases. Crystals of [Ni_2(abpy)(CH_3CN)$_2$(NO_3)$_4$] were obtained by slow vapor-diffusion of diethyl ether into the reaction mixture, whereas crystals of [Cu_2(abpy)(CH_3CN)$_8$][BF_4]$_4$ (**2**) were obtained by saturating the solution with diethyl ether and chilling it to −10 °C. The Cu^{II} compound [Cu_2(abpy)(CH_3CN)$_8$][BF_4]$_4$ (**2**) eventually decomposes to the Cu^{I} polymer {[Cu(abpy)][BF_4]$_2$}$_\infty$ (**3**) over a period of several months in toluene/acetonitrile. The identity of the reducing agent is unknown.

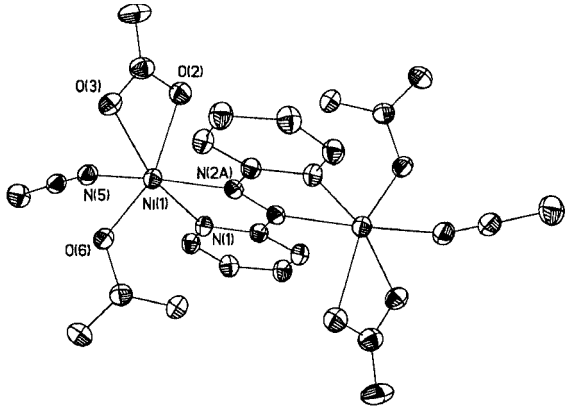

Figure 2. Thermal ellipsoid diagram (50% probability) for the dimer [Ni_2(abpy)(CH_3CN)$_2$(NO_3)$_4$] (**1**)

Electrochemical Studies

The cyclic voltammogram of **1** in acetonitrile exhibits two oxidation features at $E_{p,a}$ = +0.62V and $E_{p,a}$ = +0.4V, with no associated return waves. In addition, there are three reversible reductions located at $E_{1/2}$ = −0.10 V, $E_{1/2}$ = −0.4 V and at $E_{1/2}$ = −0.9 V. The dinuclear Cu^{II} compound **2** also exhibits a rich electrochemistry with an irreversible oxidation located at $E_{p,a}$ = +1.10 V, a reversible oxidation at $E_{1/2}$ = +0.65 V, and two reversible reductions at $E_{1/2}$ = +0.40 V and $E_{1/2}$ = 0.0 V. The fact that these reductions occur at positive potentials vs. Ag/AgCl explains why the formation of **3** is so facile.

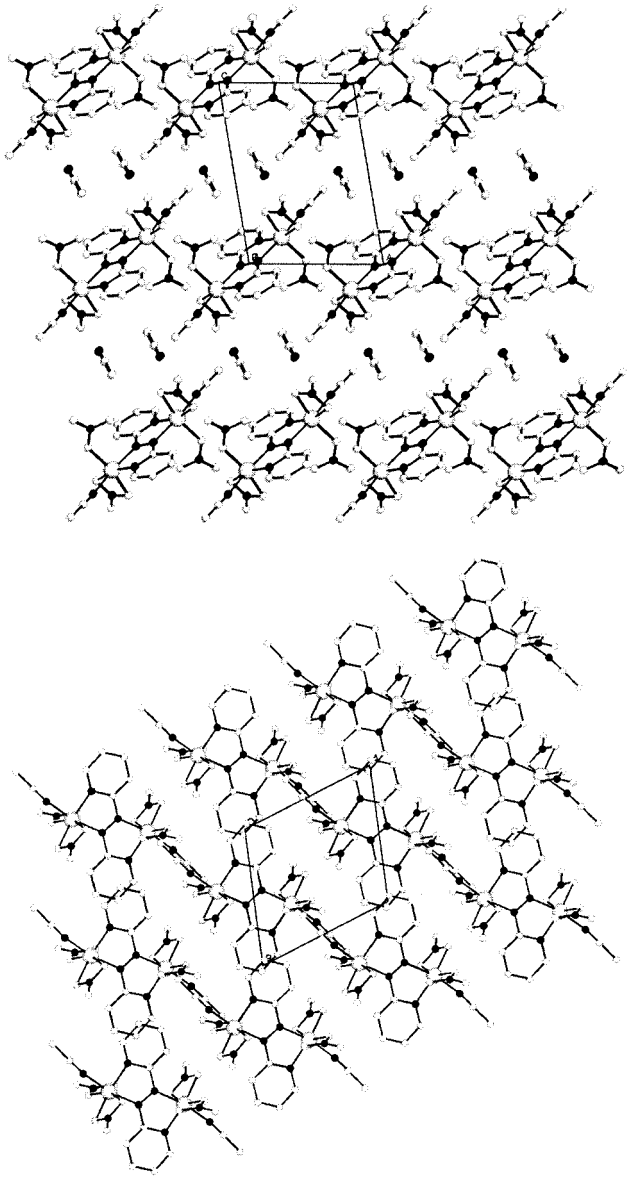

Figure 3. Projection of the packing diagram for [Ni_2(abpy)(CH_3CN)$_2$(NO_3)$_4$]·2CH_3CN (**1**·2CH_3CN) on the *ac* plane (top) and on the *bc* plane (bottom)

X-ray Crystallographic Studies

[Ni$_2$(abpy)(CH$_3$CN)$_2$(NO$_3$)$_4$]·2CH$_3$CN (1)

Crystals of [Ni$_2$(abpy)(CH$_3$CN)$_2$(NO$_3$)$_4$]·2CH$_3$CN (**1**·2CH$_3$CN) contain Ni^{II} ions in a distorted octahedral geometry (Figure 2). Each Ni center is coordinated to two [NO$_3$]$^-$ ligands — one of which acts as a bidentate ligand — as well as to an acetonitrile molecule and the bridging abpy ligand. The distortion from perfect octahedral geometry is most likely a consequence of the small bite angle of the chelating nitrate anion, which leads to an acute O−Ni−O angle of 61.43(8)° and Ni−O distances of 2.125(2) and 2.105(2) Å. The shortest Ni−L bond is with the monodentate nitrate ligand [1.990(2) Å]. The Ni−N distance to the acetonitrile ligand is 2.044(2) Å, which is essentially the same as the distance in the homoleptic solvated cation [Ni(CH$_3$CN)$_6$]$^{2+}$. The Ni−N(azo) interaction is the longest of the three Ni−N interactions [Ni(1)−N(2) = 2.121 (2) Å]. The angles within the coordination sphere also provide some helpful insight into the distortion of the ligand environment of this compound. The angle between the pyridyl and the acetonitrile ligand is close to the ideal value for an octahedron [N(5)−Ni(1)−N(1) = 93.80(2)°]. The binding angle of abpy [N(1)−Ni(1)−N(2) = 76.45(9)°] is very close to the values observed for bptz in [Ni$_2$(bptz)(CH$_3$CN)$_8$][ClO$_4$]$_4$,[4] which contains a bridging interaction involving N atoms from a pyridyl nitrogen and the tetrazine ring to give an N−Ni−N angle of 78.10 (3)°. The two Ni atoms are 4.942 Å apart, which is much shorter than the corresponding distance of 6.904 Å in [Ni$_2$(bptz)(CH$_3$CN)$_8$][ClO$_4$]$_4$. An important feature to note in the structure of **1** is the elongation of the N=N bond in the bridging abpy ligand by 0.025 Å [N(2)−N(2#) = 1.271(4) Å) relative to the corresponding distance in free abpy (1.246 Å).[27] This lengthening is indicative of π back-donation from the Ni^{II} centers into the empty π* (abpy) orbitals. This effect has been noted for a complex of abpy with Cu^I as well.[27]

In terms of intermolecular interactions, the Ni$_2$ molecules form pseudo-tetragonal layers in the *ab* plane, with solvent molecules occupying the interstices (Figure 3). There are no short contacts between the molecules, with the Ni···Ni intermolecular contacts being greater than 6 Å.

[Cu$_2$(abpy)(CH$_3$CN)$_8$][BF$_4$]$_4$ (2)

The structure of [Cu$_2$(abpy)(CH$_3$CN)$_8$][BF$_4$]$_4$ (**2**) contains the tetracationic Cu$_2$ unit, [Cu$_2$(abpy)(CH$_3$CN)$_8$]$^{4+}$, since the Cu^{II} centers are coordinated only by neutral ligands. The Cu^{II} centers exhibit a typical axial Jahn−Teller distortion, with the elongated axis oriented along the azo and acetonitrile interactions [azo: Cu(1)−N(1) 2.401(4) Å and CH$_3$CN: Cu(1)−N(12) 2.313(5) Å] (Figure 4). The other four coordination sites are filled by three acetonitrile molecules at an average Cu(1)−N distance of 2.01(5) Å, and the pyridyl ring [Cu(1)−N(2) 2.040(5) Å]. The L−Cu−L angles are distorted from the ideal octahedral values, with N(1)−Cu(1)−N(13) and N(1)−Cu(1)−N(2) being 107.0(2)° and 71.5(2)°, respectively. As noted for the Ni analogue, the longer N=N distance in the azo group [1.277 (1) Å] is indicative of π back-donation. The Cu^{II} centers are separated by a distance of 5.408 Å, which is longer that the corresponding value in the Ni^{II} compound; this situation is a consequence of the Jahn−Teller distortion.

In the Cu^{II} structure, the 3D arrangement is best described as consisting of mixed anion-cation layers in the *ab* plane separated by [BF$_4$]$^-$ anions (Figure 5). In this structure, the presence of the anions increases the intermolecular distances, with all Cu···Cu intermolecular distances being longer than 8 Å.

{[Cu(abpy)][BF$_4$]}$_\infty$ (3)

The Cu^I species,{[Cu(abpy)][BF$_4$]}$_\infty$ (**3**) is a 1-D polymer consisting of Cu^I ions connected along the *a* axis (Figure 6). The Cu^I centers exhibit a distorted tetrahedral geometry

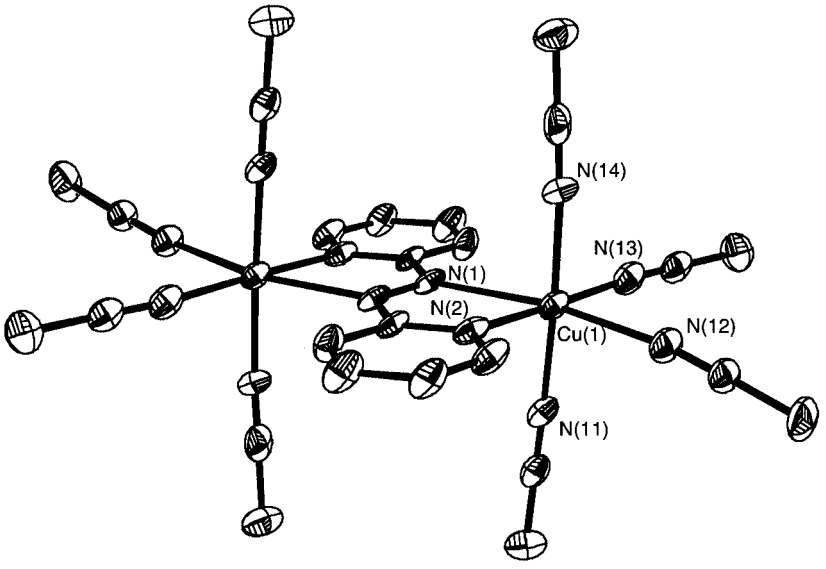

Figure 4. Thermal ellipsoid diagram (50% probability) for the dimer [Cu$_2$(abpy)(CH$_3$CN)$_8$]$^{4+}$ (**2**)

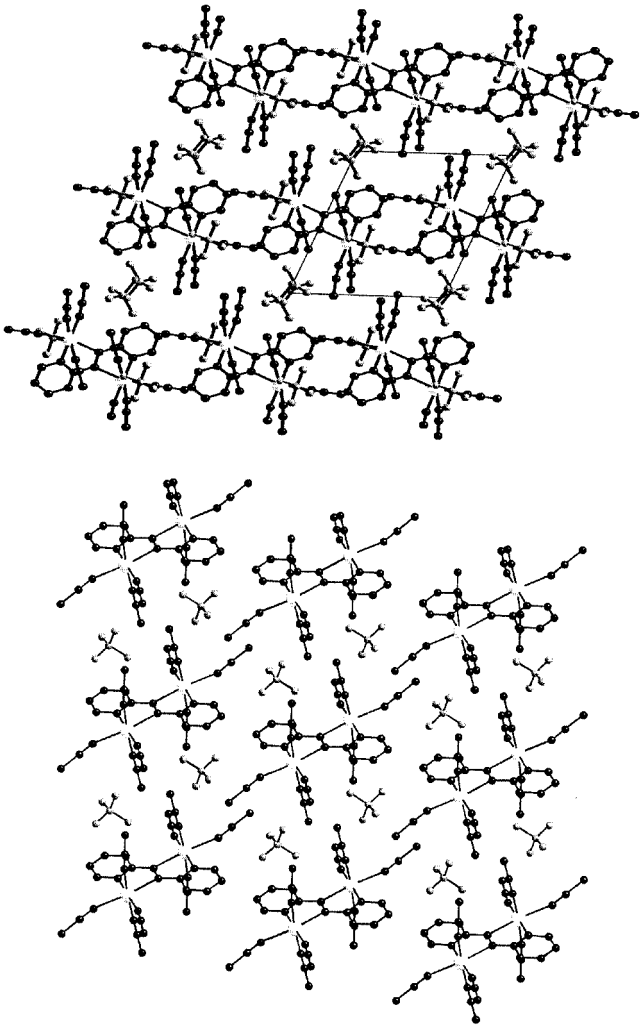

Figure 5. Projection of the packing diagram for $[Cu_2(abpy)(CH_3CN)_8][BF_4]_4$ (**2**) on the *bc* plane (top) and of the structure of one of the layers (bottom)

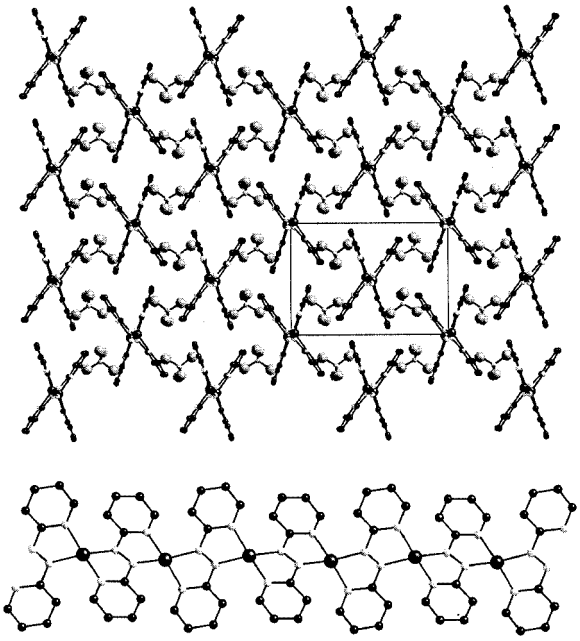

Figure 6. Projection of the packing diagram for $\{[Cu(abpy)][BF_4]\}_\infty$ (**3**) on the *bc* plane (top) and of the structure of one of the chains perpendicular to the *bc* plane (bottom)

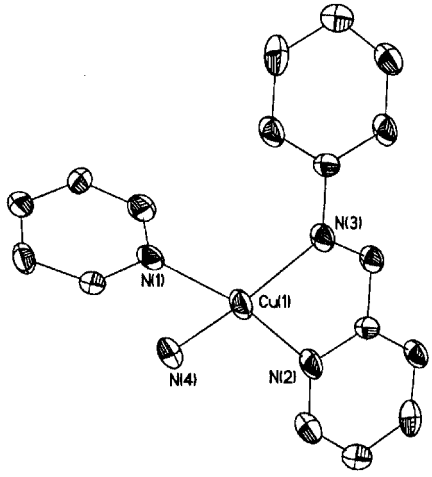

Figure 7. Thermal ellipsoid diagram (50% probability) for the monomeric building block of the $\{[Cu(abpy)]\}_\infty$ chain

(Figure 7), with the main distortions being observed due to the bite angles of the abpy ligand: N(1)−Cu(1)−N(4) = 77.7 (3)°, and N(2)−Cu(1)−N(3) = 79.4 (3)°. These angles are far from the ideal 109.5° for a tetrahedral geometry. The N(3)−N(3#) distance of 1.29(2) Å indicates that the azo group is obviously involved in appreciable π back-donation from the Cu^I, as expected for an electron-rich d^{10} center. The N=N distance is 0.054 Å longer in this compound than in free abpy, which is nearly twice the lengthening noted for the Ni^{II} and Cu^{II} complexes. The 1-D chains pack in a pseudo-hexagonal arrangement, with the counterions occupying the interstices afforded by the packing of the chains (Figure 6).

Magnetic Properties

Magnetic susceptibility measurements were performed on $[Ni_2(abpy)(CH_3CN)_2(NO_3)_4]$ (**1**) and $[Cu_2(abpy)(CH_3CN)_8][BF_4]_4$ (**2**) at 1000 G. Compound **1** shows a $\chi_m T$ value at room temperature (2.17 emu·K·mol^{-1}) that is close to the expected spin-only value for two magnetically dilute Ni centers. The $\chi_m T$ value remains constant down to 200 K (Figure 8), and then shows a steady decrease which is indicative of the presence of antiferromagnetic interactions between the $S = 1$ Ni^{II} centers. The χ versus T graph depicted in Figure 9 shows a broad maximum at 18 K which is an obvious indication that the azo bridging ligand promotes antiferromagnetic interactions. This magnetic behavior was analyzed with an isotropic model for a Ni^{II} dimer. From the Hamiltonian: $H = -2J(S1 \cdot S2)$ where $S1 = S2 = S_{Ni} = 1$, a simple expression of χ_m was derived, to which an additional paramagnetic contribution was added [Equation (1)].

The best fit to the experimental data was obtained for $g = 2.03$ and $J = -7.5$ cm^{-1}. The paramagnetic term ($C = 0.075$) accounts for about 4% of monomer impurity in the sample.

$$\chi_m = \frac{3g^2\,(2e^{2J/T}+10e^{6J/T})}{8T(1+3e^{2J/T}+5e^{6J/T})} + \frac{C}{T} \quad (1)$$

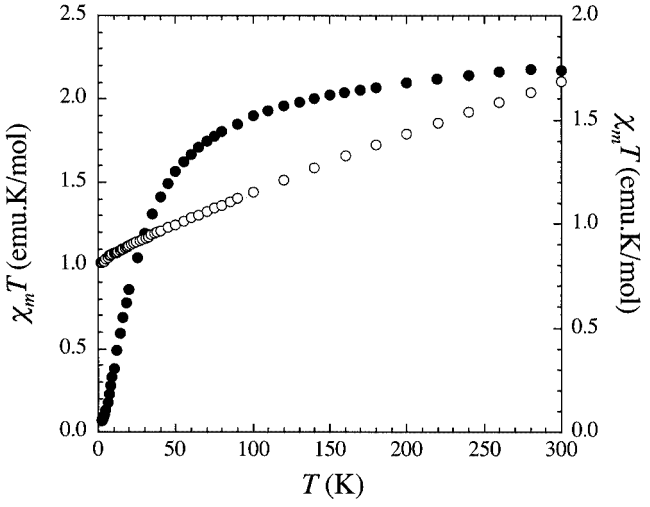

Figure 8. Plot of the $\chi_m T$ product vs. T for $[Ni_2(abpy)(CH_3CN)_2(NO_3)_4]\cdot 2CH_3CN$ (**1**, full circles) and $[Cu_2(abpy)(CH_3CN)_8][BF_4]_4$ (**2**, empty circles)

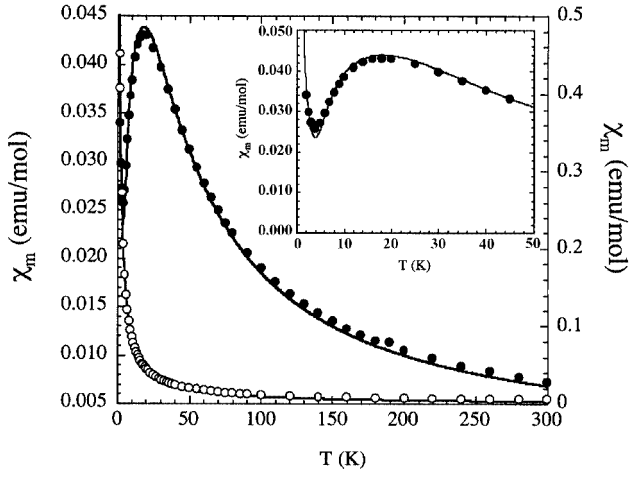

Figure 9. Plot of χ_m vs. T for $[Ni_2(abpy)(CH_3CN)_2(NO_3)_4]\cdot 2CH_3CN$ (**1**, full circles) and $[Cu_2(abpy)(CH_3CN)_8][BF_4]_4$ (**2**, empty circles); the corresponding lines represent the best fit obtained in each case

Compound **2** exhibits a $\chi_m T$ value (Figure 8) of 1.6 emu·K·mol^{-1} at room temperature, as compared to the expected spin-only value of 0.75 emu·K·mol^{-1} (for $g = 2$). The $\chi_m T$ plot gradually decreases with temperature and reaches a minimum value of 0.81 emu·K·mol^{-1} at 1.8 K. This behavior suggests the presence of a TIP (temperature-independent paramagnetism). The absence of a maximum in χ_m indicates that the magnetic interaction through the abpy ligand is small in this case. Indeed, the χ_m versus T graph (Figure 9) shows a typical exponential paramagnetic behavior. The data were fitted to a model for a Cu^{II} dimer, analogous to the one used for the Ni case, including a TIP contribution instead of a paramagnetic impurity contribution. From the expression derived for the susceptibility [Equation (2)], the fitting led to values of $g = 2.09$ and $J = -0.05$ cm^{-1}, and a TIP of 4×10^{-3} emu·mol^{-1}. These results support the conclusion that the interaction is essentially negligible in the Cu^{II} compound.

$$\chi_m = \frac{3g^2(2e^{2J/T})}{8T(1+3e^{2J/T})} + \chi_{TIP} \quad (2)$$

The fact that the magnetic interaction between Cu^{II} centers through the abpy ligand is much weaker than the corresponding interaction between Ni^{II} centers can be rationalized on the basis of geometrical considerations of the magnetic orbitals involved in the interaction, in addition to the longer distance between metal centers, when compared to the one observed for the Ni dimer. The X-ray studies reveal that the Cu^{II} centers exhibit a Jahn−Teller distortion of the axial elongation type along the N atoms of the azo group. The magnetic orbital therefore is $d_{x^2-y^2}$ which is orthogonal to the azo interaction. One would expect that superexchange through the pyridine ring and across the azo group to the adjacent pyridine ring would be very poor. Conversely, in the case of the Ni_2 compound both e_g orbitals are singly-occupied and there is no Jahn−Teller distortion. The improved overlap of the magnetic orbitals on the Ni^{II} ions with the N atoms of the bridging abpy ligand would be expected to lead to improved magnetic superexchange; this is corroborated by the magnetic measurements.

Conclusion

Two new paramagnetic dinuclear molecules were prepared by the reaction of Ni^{II} and Cu^{II} ions with the azo-2,2′-bypyridine (abpy) ligand. The compounds $[Ni_2(abpy)(CH_3CN)_2(NO_3)_4]$ and $[Cu_2(abpy)(CH_3CN)_8][BF_4]_4$ were fully characterized by X-ray crystallography, electrochemistry, electronic spectroscopy and magnetic susceptibility. The abpy ligand acts as a bridge between paramagnetic Ni^{II} and Cu^{II} centers in both cases and promotes antiferromagnetic interactions between the $S = 1$ Ni^{II} centers but does not provide a good pathway for superexchange in the $S = 1/2$ Cu^{II} dinuclear molecule. The different magnetic behavior can be explained by the fact that the Cu^{II} compound exhibits a Jahn−Teller distortion that leads to poor overlap of the magnetic orbitals through the bridging ligand.

The magnetic results allow for consideration of whether superexchange will be efficient through the abpy ligand. The antiferromagnetic exchange observed in the Ni^{II} compound is of the same order of magnitude found for ligands such as oxalate[28,29] and 2,2′-bipyrimidine.[30,31] On the ba-

Table 1. Crystallographic data and refinement parameters

	1·2CH_3CN	**2**	**3**
Formula	$C_{18}H_{20}N_{12}Ni_2O_{12}$	$C_{26}H_{32}B_4Cu_2F_{16}N_{12}$	$C_{10}H_8BCuF_4N_4$
Molecular weight	713.88	986.96	334.56
Space group	$P\bar{1}$	$P\bar{1}$	$P2_1/n$
Temperature (K)	110(2)	110(2)	110(2)
a (Å)	8.290(5)	10.240(2)	9.295(2)
b (Å)	8.343(5)	10.597(2)	9.541(2)
c (Å)	11.180(5)	10.712(2)	13.486(3)
α (deg)	105.357(5)	64.23(3)	90
β (deg)	94.387(5)	78.21(3)	91.58(3)
γ (deg)	107.564(5)	78.57(3)	90
V (Å^3)	700.5(7)	1026.7(3)	1195.5(4)
Z	1	1	4
ρ_{calc} (g/cm^3)	1.692	1.596	1.859
μ (Mo-K_α) (cm^{-1})	14.25	11.46	18.71
Reflections total/unique	8160/3252	7358/3484	11151/2040
$I > n\sigma$	2	4	4
Reflections/parameters	2815/199	2887/309	1096/133
R_1	0.0416	0.0662	0.0833
wR_2	0.1054	0.1688	0.2028
Goodness-of-fit	1.087	1.021	0.973

sis of this study, we conclude that the abpy ligand will be useful for the design of a range of magnetically interesting molecules and materials.

Experimental Section

General Remarks: All operations were performed under a nitrogen atmosphere using standard Schlenk-line techniques, unless otherwise indicated. Solvents were distilled prior to use from the appropriate drying agents. Acetonitrile was distilled from over 3 Å molecular sieves, whereas toluene and diethyl ether were distilled from over a Na/K amalgam. The reagent $Ni(NO_3)_2{\cdot}6H_2O$ was purchased from Aldrich and used without further purification. The compound $[Cu(CH_3CN)_4][BF_4]_2$ was synthesized according to published methods.[32] IR spectra were measured as Nujol mulls between KBr plates on a Nicolet 740 FT-IR spectrometer. Magnetic susceptibility measurements were performed in the range of 2−300 K with a Quantum Design SQUID magnetometer MPMS-XL. All measurements were performed on polycrystalline samples. Data were corrected for diamagnetic contributions calculated from Pascal constants.[33] The cyclic voltammetric studies were performed on a CH Instruments Electrochemical Analyzer in acetonitrile containing 0.1 M tetra-*n*-butylammonium hexafluorophosphate ([TBA][PF_6]) as the supporting electrolyte. The working electrode was a BAS Pt disk electrode, the reference electrode was Ag/AgCl and the counter electrode was a Pt wire. The Cp_2Fe/Cp_2Fe^+ couple occurs at +0.52 V vs. Ag/AgCl under the same experimental conditions.

$[Ni_2(abpy)(CH_3CN)_2(NO_3)_4]$ (1): A sample of $Ni(NO_3)_2{\cdot}6H_2O$ (100 mg, 0.34 mmol) was dissolved in 30 mL of acetonitrile to give a pale green solution which was stirred until the entire solid had dissolved, after which time abpy (32 mg, 0.17 mmol) was added. The resulting intensely green solution was stirred for 4 additional hours and then concentrated to 10 mL. Slow vapor diffusion of diethyl ether into the reaction solution afforded dark green crystals within 6 days. Yield = 80 mg (75%). IR (KBr): $\tilde{\nu}$ = 2724 cm^{-1} (w), 1620 (w), 1147 (w), 1039 (w), 1022 (w), 801 (w), 722 (w). UV/Vis (acetonitrile, $c = 9.8 \times 10^{-6}$ M): λ = 344 nm [$\varepsilon = 1.8 \times 10^4$ L(mol·cm)$^{-1}$].

$[Cu_2(abpy)(CH_3CN)_8][BF_4]_4$ (2): A sample of $[Cu(CH_3CN)_4][BF_4]_2$ (100 mg, 0.249 mmol) was dissolved in 20 mL of acetonitrile and treated with abpy (22 mg, 0.124 mmol). A color change from blue to pale green quickly ensued. The reaction mixture was stirred overnight, concentrated and treated with diethyl ether to the point of saturation. Light green platelet crystals of **2** were obtained by placing the solution in the freezer at −4 °C for a week. Yield = 82 mg (80%). IR (KBr): $\tilde{\nu}$ = 2724 cm^{-1} (w), 2296 (w), 2323 (w), 1589 (w), 1261 (w), 1229 (w), 1027 (br,s), 805 (w), 722 (w). UV/Vis (acetonitrile, $c = 8.0 \times 10^{-6}$ M): λ = 351 nm [$\varepsilon = 2.7 \times 10^4$ L(mol·cm)$^{-1}$], 230 [$\varepsilon = 1.98 \times 10^4$ L(mol·cm)$^{-1}$].

$\{[Cu(abpy)][BF_4]\}_\infty$ (3): A solution of **2** in acetonitrile layered with toluene produced dark green needle-like crystals of **3** after a period of one month.

X-ray Crystallographic Study: The X-ray data sets were collected on a SMART 1 K area detector diffractometer equipped with graphite monochromated Mo-K_α radiation (λ = 0.71073 Å). The frames were integrated with the Siemens SAINT[34] software package and the data were corrected for absorption using the SADABS program.[35] The structures were solved using the direct-methods programs SHELXS-97 (**1** and **3**),[36] and SIR97 (**2**). Crystal parameters and basic information pertaining to data collection and refinement are summarized in Table 1.

A dark green prismatic crystal of **1** was secured on the tip of a glass fiber with Dow Corning silicone grease and placed in a cold N_2(g) stream at 110 (2) K. A total of 8160 reflections were collected of which 3252 were unique. The final refinement cycle was based on 2815 reflections with $F_0 > 2\sigma(F_0)$ ($R1$ = 0.0416 and $wR2$ = 0.1054).

A light green platelet of **2** was secured on the tip of a glass fiber with Dow Corning silicone grease and placed in a N_2(g) stream at 110 (2)K. The data collection involved a total of 7358 reflections of which 3484 were unique. The final refinement cycle was based

on 2887 reflections with $F_0 > 4\sigma(F_0)$ that were used to fit 309 parameters which led to $R1 = 0.0662$ and $wR2 = 0.1688$. The goodness-of-fit index is 1.021, and the highest peak in the final difference map is 1.195 $e^-\cdot Å^3$.

A green needle-like crystal of **3** was covered with Paratone oil, secured on the tip of a glass fiber with Dow Corning silicone grease, and placed under a N_2(g) stream at 110 (2)K. A total of 11151 reflections were collected of which 2040 were unique. The final refinement cycle was based on 1096 reflections with $F_0 > 4\sigma(F_0)$ that were used to fit 181 parameters which led to $R1 = 0.0833$ and $wR2 = 0.2028$. The goodness-of-fit index is 0.973, and the highest peak in the final difference map is 1.765 $e^-\cdot Å^3$.

CCDC 183947 (**1**), -183948 (**2**) and -183949 (**3**) contain the supplementary crystallographic data for this paper. These data can be obtained free of charge at www.ccdc.cam.ac.uk/conts/retrieving.html [or from the Cambridge Crystallographic Data Centre, 12, Union Road, Cambridge CB2 1EZ, UK; fax: (internat.) +44-1223/336-033; E-mail: deposit@ccdc.cam.ac.uk].

Acknowledgments

We thank the National Science Foundation for a PI grant (CHE-9906583) and for equipment grants for the CCD X-ray equipment (CHE-9807975) and the SQUID magnetometer (NSF-9974899). Support from the Welch Foundation is also gratefully acknowledged. JRGM thanks the Spanish Ministerio de Ciencia y Tecnología for a research contract (Programa Ramón y Cajal).

[1] O. Kahn, C. J. Martinez, *Science* **1998**, *279*, 44−48.
[2] C. Joachim, J. K. Gimzewski, A. Aviram, *Nature* **2000**, *408*, 541−548.
[3] J. M. Tour, *Acc. Chem. Res.* **2000**, *33*, 791−804.
[4] C. S. Campos-Fernandez, R. Clérac, K. R. Dunbar, *Angew. Chem. Int. Ed.* **1999**, *38*, 3477−3479.
[5] C. S. Campos-Fernandez, R. Clérac, J. M. Koomen, D. H. Russell, K. R. Dunbar, *J. Am. Chem. Soc.* **2001**, *123*, 773−774.
[6] J. R. Galán-Mascarós, K. R. Dunbar, *Chem. Commun.* **2001**, 217−218.
[7] A. Aumüller, P. Erk, G. Klebe, S. Hünig, J. Schütz, H. Werner, *Angew. Chem. Int. Ed. Engl.* **1986**, *25*, 740−741.
[8] P. Erk, H. J. Gross, U. L. Hünig, H. Meixner, J. U. Von Schütz, H. C. Wolf, *Angew. Chem. Int. Ed. Engl.* **1989**, *28*, 1245−1246.
[9] M. L. Naklicki, R. J. Crutchley, *J. Am. Chem. Soc.* **1994**, *116*, 6045−6046.
[10] R. Kato, H. Kobayashi, A. Kobayashi, *J. Am. Chem. Soc.* **1989**, *111*, 5224−5232.
[11] W. Kaim, S. Kohlmann, *Inorg. Chem.* **1987**, *26*, 68−77.
[12] W. Kaim, S. Kohlmann, *Inorg. Chem.* **1986**, *25*, 3442−3448.
[13] H. Hartmann, T. Scheiring, J. Fiedler, W. Kaim, *J. Organomet. Chem.* **2000**, *604*, 267−272.
[14] S. Ernst, V. Kasack, W. Kaim, *Inorg. Chem.* **1988**, *27*, 1146−1148.
[15] S. Ernst, W. Kaim, *Inorg. Chem.* **1989**, *28*, 1520−1528.
[16] W. Kaim, S. Ernst, V. Kasack, *J. Am. Chem. Soc.* **1990**, *112*, 173−178.
[17] L. S. Kelso, D. A. Reitsma, R. Keene, *Inorg. Chem.* **1996**, *35*, 5144−5153.
[18] S. I. Gorelsky, E. S. Dodsworth, A. B. P. Lever, A. A. Vlcek, *Coord. Chem. Rev.* **1998**, *174*, 469−494.
[19] S. Kohlman, S. Ernst, W. Kaim, *Angew. Chem. Int. Ed. Engl.* **1985**, *24*, 684−685.
[20] W. Kaim, *Coord. Chem. Rev.* **2001**, *219−221*, 463−488.
[21] D. A. Baldwin, A. B. P. Lever, R. V. Parish, *Inorg. Chem.* **1969**, *8*, 107−115.
[22] W. Kaim, S. Kohlmann, J. Jordanov, D. Fenske, *Z. Anorg. Allg. Chem.* **1991**, *598−599*, 217−234.
[23] P. Kausikisankar, M. Shivakumar, P. Ghosh, A. Chakravorty, *Inorg. Chem.* **2000**, *39*, 195−199.
[24] E. Waldhör, J. Poppe, W. Kaim, E. Cutin, M. García, N. Katz, *Inorg. Chem.* **1995**, *34*, 3093−3096.
[25] A. J. Bellamy, I. S. MacKirdy, C. E. Niven, *J. Chem. Soc., Perkin. Trans. 2* **1983**, 183−185.
[26] M. B. Robin, P. Day, *Adv. Inorg. Chem. Radiochem.* **1967**, *10*, 247−422.
[27] R. Schäfer, W. Kaim, J. Fiedler, *Inorg. Chem.* **1993**, *32*, 3199−3200.
[28] E. Coronado, J. R. Galán-Mascarós, C. J. Gómez-García, *J. Chem. Soc., Dalton Trans.* **2000**, 205−210.
[29] E. Coronado, J. R. Galán-Mascarós, C. Giménez-Saiz, C. J. Gómez-García, C. Ruiz-Pérez, S. Triki, *Adv. Mater.* **1996**, *8*, 737−740.
[30] S. Triki, F. Thetiot, J. R. Galán-Mascarós, J. Sala-Pala, K. R. Dunbar, *New J. Chem.* **2001**, *25*, 954−958.
[31] G. De Munno, G. Viau, M. Julve, F. Lloret, J. Faus, *Inorg. Chim. Acta* **1997**, *257*, 121−129.
[32] B. J. Hathaway, D. G. Holah, A. E. Underhill, *J. Chem. Soc.* **1962**, 2444−2448.
[33] *Theory and Applications of Molecular Paramagnetism* (Eds.: E. A. Boudreaux, L. N. Mulay), John Wiley & Sons: New York, 1976.
[34] SAINT, Program for area detector absorption correction, Siemens Analytical X-ray Instruments Inc., Madison WI 53719, USA 1994−1996.
[35] Program in the SHELXTL software.
[36] SHELXL-97; G. M. Sheldrick, SHELXL-97, Program for refining crystal structures, University of Göttingen,1997.

Received May 13, 2002
[I02253]